



Functional neural network configuration in late childhood varies by age and cognitive state

Thang M. Le^{a,*}, Anna S. Huang^b, Jonathan O'Rawe^c, Hoi-Chung Leung^{c,**}

^a Department of Psychiatry, Yale University School of Medicine, New Haven, CT 06519, USA

^b Department of Psychiatry and Behavioral Sciences, Vanderbilt University School of Medicine, Nashville, TN 37212, USA

^c Department of Psychology, Integrative Neuroscience Program, Stony Brook University, Stony Brook, NY 11790, USA

ARTICLE INFO

Keywords:

Late childhood
Network connectivity
Integration
Flexibility
Cognitive processing
Age effect

ABSTRACT

Late childhood and early adolescence is characterized by substantial brain maturation which contributes to both adult-like and age-dependent resting-state network connectivity patterns. However, it remains unclear whether these functional network characteristics in children are subject to differential modulation by distinct cognitive demands as previously found in adults. We conducted network analyses on fMRI data from 60 children (aged 9–12) during resting and during three distinct tasks involving decision making, visual perception, and spatial working memory. Graph measures of network architecture, functional integration, and flexibility were calculated for each of the four states. During resting state, the children's network architecture was similar to that in young adults ($N = 60$, aged 20–23) but the degree of similarity was age- and network-dependent. During the task states, the children's whole-brain network exhibited enhanced integration in response to increased cognitive demand. Additionally, the frontoparietal network showed flexibility in connectivity patterns across states while networks implicated in motor and visual processing remained relatively stable. Exploratory analyses suggest different relationships between behavioral performance and connectivity profiles for the working memory and perceptual tasks. Together, our findings demonstrate state- and age-dependent features in functional network connectivity during late childhood, potentially providing markers for brain and cognitive development.

1. Introduction

Late childhood and early adolescence marks a crucial development period characterized by the substantial maturation of functional brain networks and the emergence of complex cognitive abilities (Casey et al., 2005; Steinberg, 2005). Recent network analyses using resting-state functional connectivity (rsFC) revealed increasing long-range connections (Betzel et al., 2014; Lee et al., 2013), stronger cortico-cortical connectivity (Baker et al., 2015), and more well-defined networks (Grayson et al., 2014) with age. Concurrently, cognitive domains including working memory, decision making, and cognitive flexibility also undergo substantial improvement during this period (Dajani and Uddin, 2015; Shing et al., 2010; Zelazo and Carlson, 2012). A link between brain network and cognitive development has been recently suggested. For instance, stronger rsFC in core neurocognitive networks, specifically the frontoparietal network (FPN), has been associated with better working memory (Li et al., 2013), executive function (Lin et al.,

2015), and reading competence (Koyama et al., 2011) in children. Nevertheless, few studies examined the direct relationship between task-state network connectivity and behavioral performance in children. Furthermore, a feature of the mature neural networks during cognitive processing is the ability to respond differentially in connectivity patterns to different tasks and yet flexibly switch between them when cognitive demand changes (Cole et al., 2013; Shirer et al., 2012). Whether such ability is present or to what extent it is present in late childhood and early adolescence, however, remains poorly understood.

In response to increased cognitive demand, functional networks in adults exhibit greater connection strength and density across distributed brain regions. This enhancement, referred to as integration, is quantified by several graph metrics including modularity and global efficiency (see *Methods*) (Rubinov and Sporns, 2010). For instance, whole-brain network exhibited more efficient and less modular connectivity patterns during the cognitively demanding n-back task relative to finger tapping or resting (Cohen and D'Esposito, 2016; Shine et al., 2016).

* Corresponding author at: Connecticut Mental Health Center, S105 34 Park Street, New Haven, CT 06519-1109, USA.

** Corresponding author at: Stony Brook University, Department of Psychology, Stony Brook, NY 11794-2500, USA.

E-mail addresses: thang.le@yale.edu (T.M. Le), hoi-chung.leung@stonybrook.edu (H.-C. Leung).

<https://doi.org/10.1016/j.dcn.2020.100862>

Received 11 August 2019; Received in revised form 31 July 2020; Accepted 26 August 2020

Available online 8 September 2020

1878-9293/© 2020 The Author(s).

Published by Elsevier Ltd.

This is an open access article under the CC BY-NC-ND license

(<http://creativecommons.org/licenses/by-nc-nd/4.0/>).

Such task-induced integration is postulated to reflect the convergence of information from diverse brain sources to support complex cognition (Shine and Poldrack, 2017; Sporns, 2013). In late childhood, developmental characteristics of functional networks may significantly impact integration as distal connection density and modularity during resting have been shown to be lower in children than adults (Gao et al., 2009; Miskovic et al., 2015). Abnormalities in integration can also affect cognition as attenuated frontoparietal connectivity during working memory (Koshino et al., 2005) and reduced global efficiency in the default mode network (DMN) at rest (Wang et al., 2009) were associated with poor cognitive outcomes in autism and attention deficit hyperactivity disorder. Thus, better understanding of network properties such as the degree of integration during task performance in children may provide insights into the typical as well as atypical developmental trajectories of brain and cognition.

As tasks involving different cognitive demands can elicit distinguishable patterns of network connectivity (Cole et al., 2013; Shirer et al., 2012), the transition from one cognitive state to another (e.g., resting to task) likely elicits changes in connectivity patterns, necessitating adaptive flexibility in functional neural network configuration (Bassett and Gazzaniga, 2011; Davison et al., 2015). Flexibility in shifting functional connectivity patterns across tasks has been recently quantified by graph measures involving the variability in nodal membership, connectivity strength, and network configuration (see *Methods*) (Bassett et al., 2010, 2015a; Cole et al., 2013). The FPN has been shown to be particularly flexible, demonstrated by highly variable connectivity patterns across tasks of distinct demands including learning, decision making, inhibitory control, and motor responses (Cole et al., 2013; Spielberg et al., 2015). Flexibility is likely reflective of cognitive abilities. In adults, greater flexibility, as measured by connectivity variability and changes in nodal memberships between different neural networks, predicted higher behavioral flexibility (Nomi et al., 2017) and faster skill acquisition in a motor task (Bassett et al., 2010), respectively. Both cognitive demand and age have been shown to influence variability in neural activity, with greater variability reported in tasks relative to resting and in young relative to older adults (Garrett et al., 2013). In late childhood, behavioral studies have reported children's ability to flexibly switch between distinct tasks (Chevalier and Blaye, 2009; Davidson et al., 2006). Yet, given the relatively slow gray matter maturation of the FPN in children (Gogtay et al., 2004), the neural basis for such behavioral variability is still unknown.

As functional network connectivity in late childhood is subject to the influence of both cognitive demand and brain development, we sought to characterize how functional networks respond to distinct cognitive tasks and how such responses may vary by age. Using graph theory, we examined functional network properties in children aged between 9 and 12 during resting and three task states involving rewarded decision making, visual perception, and working memory. The three tasks were designed to tap into several distinct cognitive and sensory domains, recruiting various brain networks associated with motivational, working memory, perceptual, and motor processing. The whole-brain network architecture (i.e., the brain organization into functional network modules of highly interconnected regions) was defined for each state. The intrinsic (i.e. resting) architecture was compared to that of an adult sample to quantify potential age effects. We tested the hypothesis that the intrinsic network architecture in children would be broadly similar to that in adults although this similarity would vary with age and modules, the latter of which is likely due to the different neuronal maturation rates across the cerebral cortex. Next, we examined whether whole-brain functional integration as well as network module flexibility were modulated by task demand. We hypothesized that greater integration would be associated with increasing cognitive demand in children, while anticipating the degree of integration to be both task- and age-dependent. Among neurocognitive networks including the FPN, Salience, DMN, Visual, and Somatomotor (SMN) networks, (Dosenbach et al., 2006; Bassett et al., 2010; Duncan, 2010), those implicated in

executive function or multimodal processing were hypothesized to exhibit a high degree of flexibility.

2. Materials and methods

2.1. Data samples

Eighty children recruited from a larger study investigating individuals with and without parental history of depression (Kujawa et al., 2012) participated in one fMRI session. During the session, participants performed resting, a reward task, a visual perception task, and a spatial working memory task. We analyzed a subset of the sample after excluding data with excessive head motion in at least one of the fMRI sessions (20 participants) and failures to follow task instructions (8 participants). For the final analysis, a total of 60 participants (28 females, age 9–12, mean \pm SD: 10.72 \pm .88 years) with usable resting state fMRI data were used in the community detection analysis to define the intrinsic network architecture; and a total of 52 participants (27 females, 10.77 \pm .90 years) with complete fMRI data for all four task states were used in the analysis of network properties. The Pubertal Development Scale was used to measure puberty score at the time of fMRI. The participants had a mean puberty score of 8.37 \pm 2.36 (data was missing from one male). Female and male participants did not significantly differ in their PDS scores ($p = .067$). Informed consent was obtained from parents of subjects prior to participation in accordance to the Stony Brook University Institutional Review Board.

For comparison, we used a subsample of 60 young adults from the Cambridge Buckner 1000 Connectomes Project dataset (referred to as CB sample from here on) (Biswal et al., 2010). These subjects (age 20–23, mean 21.2 years) were selected to match the age variance in our child sample.

2.2. Tasks during fMRI

Resting: Resting state fMRI data were acquired in two runs (11 min 52 s total), during which participants were instructed to relax and look at the center of a target covering the whole screen. Resting-state sessions were performed prior to the task-state sessions.

Reward task (Fig. 1A): On each trial, after a 2-s fixation, two doors were displayed on the screen for 2 s and participants were instructed to indicate their choice by pressing the left or right button. After an 800-ms fixation, feedback of monetary gain (“You Win”) or loss (“You Lose”) was displayed for 1.2 s. There was a total of 60 trials (30 win, 30 loss), with win/loss trials in a pseudorandom order. The intertrial interval (ITI) was jittered (mean: 2.5 s, range: 0–14 s), with an average trial duration of 8 s. There were 2 runs with each run lasting 4 min 20 s.

Perception task (Fig. 1B): There were 4 different block conditions: neutral faces, sad faces, happy faces, and houses. Each block was 16-s long and contained 4 trials. At the beginning of each block, a 1-s warning fixation changed in color from black to blue to cue the start of the block. On each trial, a 600-ms fixation cross was followed by the simultaneous presentation of two images for 3000 ms, either two faces or two houses and participants made a button press to indicate whether the two images were identical or different (50/50 chance). There were 3 blocks per condition, presented in a pseudorandom order. These task blocks were interleaved with 14 s of fixation. The run lasted 6 min and 12 s.

Working memory task (Fig. 1C): We used a 1-back spatial working memory paradigm with two load conditions (Load 1 and Load 3). One rabbit was presented in the Load 1 condition, whereas three rabbits in three different locations were presented in the Load 3 conditions; rabbits were positioned pseudorandomly around an invisible circle with a radius of 5° visual angle. The two load conditions were presented in blocks of 5 trials. On each trial except the first trial of each block, participants pressed a button to indicate whether any rabbit was in a different location from the previous trial. In the Load 3 condition, one of

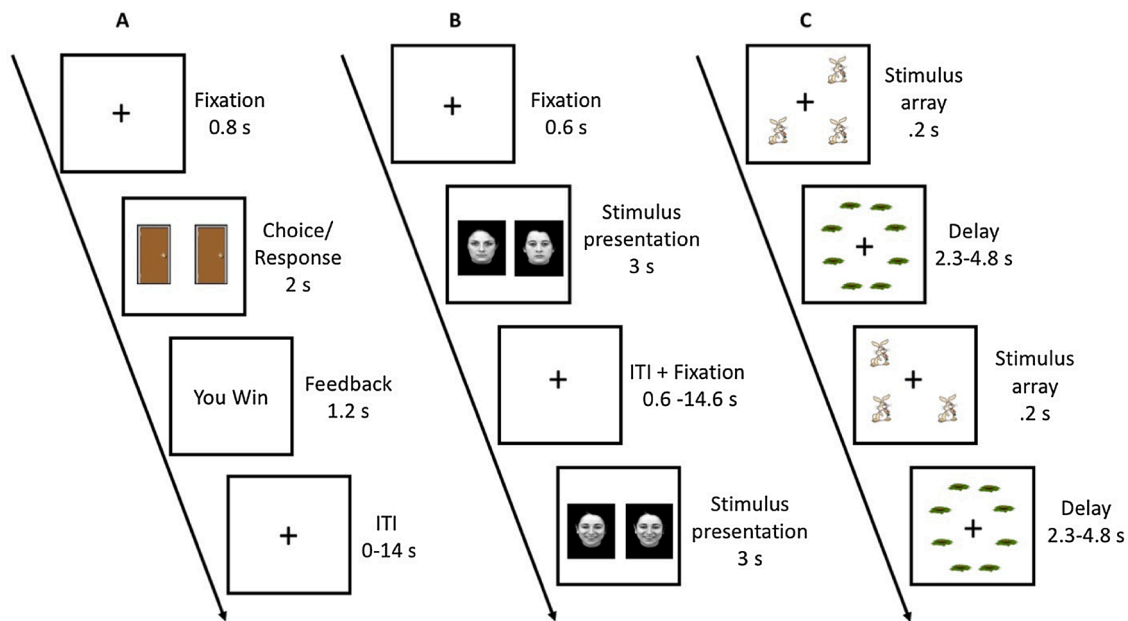


Fig. 1. Behavioral tasks. Participants performed three cognitive tasks during fMRI. (A) In the reward task, upon presented with 2 doors, participants were instructed to choose either the one on the left or on the right. Monetary gain (shown in figure) or loss (50:50 chance) was indicated by visual feedback. (B) In the perception task, two images, either of faces (shown in figure) or houses, were presented to participants who were instructed to determine by a button press whether the images were identical or not. (C) In the working memory task, either 1 or 3 (shown in figure) rabbits were shown. Participants were instructed to determine whether the rabbits were in the same locations as the immediately preceding trial.

the rabbits changed location on a change trial. The rabbits were presented for 200 ms. There were 8 possible locations shifted between 5° to 10° from regular clock orientation. Locations were masked with 8 rabbit holes (average 1° visual angle) presented during a variable ITI of 2.3, 3.3 or 4.8 s (average 3.2 s). Each task block lasted 17 s with a 13-s fixation period between blocks. There were two runs of 4 min 12 s each (8 blocks/run).

To ensure task compliance and minimize head and body motion during the experiment, each child practiced all tasks and participated in a training session prior to scanning. During the training session, participants were positioned in a mock scanner to become acclimated with the scanner environment (e.g., spatial dimensions, sounds, lighting etc.). In the mock scanner, a motion sensor worn on the participants' forehead and connected to a computer screen was used to visually demonstrate the magnitude of movements in real time. The children were given feedback when their movements exceeded the set motion threshold (see below). Due to computer software malfunctions, behavioral data were only recorded during the working memory and perception task for 35 and 39 participants, respectively. Thus, while fMRI data were available and analyzed for all 52 individuals, behavioral analyses were only performed on the subset of those participants.

2.3. Data acquisition and analysis

2.3.1. Imaging parameters

Data were collected on a 3 T Siemens Tim Trio whole-body MRI system (Erlangen, Germany). Whole-brain structural anatomical images were acquired in the sagittal plane with a T1 weighted MPRAGE scanning sequence (TR = 2400 ms; TE = 3.16 ms; slices = 176; flip angle = 8° ; FOV = 256×256 ; matrix = 256×256 ; resolution = $1 \times 1 \times 1 \text{ mm}^3$). T2-weighted structural images were collected in the axial oblique plane parallel to the AC-PC (TR = 6450; TE = 88; slices = 37, 3.5 mm with no gap; flip angle = 120° ; FOV = 256×256 ; matrix = 256×256 ; resolution = $1 \times 1 \times 3.5 \text{ mm}^3$). Two runs of resting state (175 volumes each), two runs of the reward task (123 volumes each), one run of the perception task (183 volumes), and two runs of the working memory task (127 volumes each) were acquired in the axial oblique plane

parallel to the AC-PC with a T2*-weighted single-shot echo-planar pulse sequence (TR = 2000 ms; TE = 30 ms; slices = 37; flip angle = 90° ; FOV = 224×224 ; matrix = 64×64 ; resolution = $3.5 \times 3.5 \times 3.5 \text{ mm}^3$). Each session began with 3 dummy scans which were discarded prior to data analysis.

For the adult data sample, structural images were acquired using the MPRAGE sequence: slices = 192, matrix size = 144×192 , resolution = $1.20 \times 1.00 \times 1.33 \text{ mm}^3$. Resting state T2*-weighted axial images were acquired using the EPI sequence: 47 interleaved axial slices, TR = 3000 ms, resolution = $3.0 \times 3.0 \times 3.0 \text{ mm}^3$ (119 volumes, interleaved slices).

2.3.2. Image preprocessing

Images were preprocessed with SPM12 (Wellcome Trust Centre for Neuroimaging). Standard preprocessing steps were applied to each dataset including slice timing correction, volume alignment for motion correction, and co-registration of anatomical to the mean EPI image. A unified segmentation algorithm was applied to the high-resolution structural images to separate the gray matter, white matter, and CSF. The functional and anatomical images were then spatially normalized and transformed into the MNI space, using affine nonlinear transformation, and then spatially smoothed with a 4-mm full-width at half-maximum Gaussian kernel.

As head motion can influence measures of functional connectivity, especially in children (Satterthwaite et al., 2012), we employed several measures to reduce the potential influence of motion-related artifact in the data. First, movement was visually inspected and calculated using the Artifact Detection Tools (ART, www.nitrc.org/projects/artifact_detection/). Runs with significant motion ($> 3\text{-mm}$ translation peak-to-peak movement and/or 1.5° rotation) and significant change in signal global mean ($> 3\text{SD}$) were removed. Outlier volumes were identified for frame-to-frame displacement that exceeded 0.5 mm and/or rotation $> 1.5^\circ$. On average, 94.3 % of all volumes were retained across runs and across subjects. Second, prior to assessing the functional connectivity, additional preprocessing steps were performed. A nuisance regression was constructed to control for the following confounding variables: 6 motion parameters up to their second derivatives, volumes with excessive motion, modeled physiological signal generated through aCompCor

(Behzadi et al., 2007) of the white matter and CSF voxels, and the linear drift. For resting state data, the residuals of this regression were then filtered utilizing a bandpass between the frequencies of 0.008 and 0.09 Hz and despiked using the CONN toolbox (<https://www.nitrc.org/projects/conn>). For the task state data, similar to a previous study (Cole et al., 2014), no low pass filter was applied (i.e., bandpass = .008 Hz - Inf) to preserve the possible presence of task signals at higher frequencies than the relatively slow resting-state fluctuations. Finally, to rule out the possibility head motion may have impacted network measures, we calculated the rate of change of BOLD signal across the entire brain at each frame of data (DVARS) and framewise displacement (FD) (Power et al., 2012) for each resting and task state in each subject. We then examine the relationship between DVARS/FD and measures of network properties (see *Results*).

We chose not to regress out the global signal in order to retain the interpretability of negative correlations (Murphy et al., 2009). In addition, to reduce potential influence of transient task-related effects, all visual and motor events were treated as events of no interest in a standard general linear model regression. The residuals from these regression models were used to estimate functional connectivity during the tasks. Only relevant task blocks were included in the time series (i.e., no fixation blocks), with 6 s of hemodynamic delay accounted for, and concatenated prior to correlation calculation.

2.3.3. Functional connectivity

We first conducted Pearson correlations between time series in all pairs of regions from the commonly used 264 cortical and subcortical regions-of-interest (ROIs) atlas from Power et al. (2011). ROIs were spheres of 5-mm radius centered at the coordinates as previously performed in similar analyses (Cohen and D'Esposito, 2016; Cole et al., 2014). Correlation coefficients were Fisher's Z transformed and used for all subsequent computations. As there is no clear consensus on the treatment of task events, we conducted another set of analyses without the removal of task events and produced similar results, as expected from previous reports (Cohen and D'Esposito, 2016). Here, we chose to report the findings with task events removed.

Community Detection. To determine the network architecture during resting-state, we used the Louvain community detection algorithm with two free parameters to partition the 264 ROIs into functional modules (i.e., networks of highly interconnected brain regions). The density parameter determines the threshold of connection strength. Connections with strength below this threshold were removed prior to community detection. The structural resolution parameter was used to restrict the number of communities identified in the functional connectivity matrix. To be consistent with previous work (Cole et al., 2014), we applied the same range for density threshold (40 % to 2 % in steps of 2.5) and resolution (0–3 in steps of 0.2). Each set of parameters was evaluated based on the resulting partition. The parameters were considered superior if they successfully partitioned the ROIs into functional modules as previously identified in the literature (Power et al., 2011). As such, optimal density threshold of 0.045 and resolution of 2.2 were chosen as they produced a twelve-community partition similar to Power et al. (2011).

The optimal parameters obtained from resting-state community detection were subsequently applied to the task data to identify communities in the three task states. As the Louvain algorithm is stochastic, we ran this algorithm 150 times to obtain 150 partitions. These partitions were then used to create an agreement matrix which was subjected to consensus clustering (Lancichinetti et al., 2009) to yield a final partition for each subject and each task state.

To examine architectural changes within each module across the four cognitive states, community detection was applied to key neuro-cognitive modules including FPN, salience, DMN, visual, and SMN using data from each of the four states. These networks represent the cognitive and sensory domains likely recruited by the different cognitive demands engaged during the performance of the three distinct tasks. Changes in network architecture across states, both at the whole-brain and module

levels, were quantified by adjusted Rand index (ARI) (Arabie and Hubert, 1985) which measures the similarity between two partitions while accounting for chance of similarity due to randomness. We calculated the partition similarity between the child and the CB samples to delineate potential age effects. Brain network graphs were visualized with BrainNet Viewer (Xia et al., 2013).

2.3.4. Integration metrics

At the whole-brain level, we examined the degree of integration changes in network connectivity between the resting and the three task states. Brain Connectivity Toolbox (Rubinov and Sporns, 2010) (<https://sites.google.com/site/bctnet/>) and custom MATLAB scripts were used to calculate these measures. Connectivity matrices were thresholded with the density of 0.045 (as determined by community detection optimization) prior to obtaining the graph metrics.

For the measures of integration, we used global efficiency, local efficiency, participation coefficient, number of connector hubs, and modularity. Global efficiency is the measure of average inverse shortest path length between nodes within a network (Latora and Marchiori, 2001), with higher global efficiency indicative of stronger connections between modules or high degree of integration. Global efficiency is defined as follows:

$$E_{\text{global}} = \frac{1}{N(N-1)} \sum_{i \neq j \in G} \frac{1}{L_{ij}}$$

where L is the minimum path length, N is the number of nodes in graph.

Local efficiency is the global efficiency computed on neighboring nodes (i.e., the inverse of the average shortest path connecting all neighbors of that node), with high local efficiency indicative of low integration.

Participation coefficient refers to the measure of diversity of inter-modular connections of individual nodes. A network with high participation coefficient contains nodes that have dense connections with other networks and is thus more integrated. Participation coefficient is defined as follows:

$$PC_i = 1 - \frac{\sum_{s=1}^{N_M} \left(\frac{k_{is}}{k_i}\right)^2}{N_M}$$

where k_{is} is the degree (number of connections) of node i to other nodes in its own network (s), and k_i is the degree of node i regardless of network membership.

A connector hub is a node that displays a high-degree of diverse inter-modular connectivity (van den Heuvel and Sporns, 2013). Here, connector hubs were defined as nodes with high participation coefficient (>0.8) and low within-module degree (<1.5) (Guimerà and Nunes Amaral, 2005a, 2005b). An increase in the number of connector hubs reflects an increase in integration.

Modularity is the degree to which the network may be subdivided into non-overlapping groups of nodes such that the number of within-group edges is maximized while the number of between-group edges is minimized. A high modular configuration indicates a low degree of integration. Modularity is defined as follows:

$$Q = \sum_{n=1}^m (e_{ii} - x_i^2)$$

where e_{ii} is the fraction of all edges connecting two nodes within module n , x_i is the fraction of edges connecting a node in module i to any other node, and m represents the total number of modules.

2.3.5. Flexibility metrics

At the module level, we assessed the flexibility of connectivity pattern for the five functional modules across the four cognitive states. Flexibility refers to the degree of change in connectivity patterns of a

network across multiple states. Specifically, we used connectivity variability, nodal membership change, and module partition similarity. Connectivity variability is the variability in connectivity strength measured by standard deviation across the four cognitive states (Cole et al., 2013). High variability indicates a high degree of flexibility.

Nodal membership change is the probability of a node switching its membership to a different module upon transition from one state to another, calculated by the number of times a node changes membership normalized by the total possible number of changes (Bassett et al., 2010). To avoid potential bias for/against any network(s) or state(s), nodal membership changes were averaged across the three resting-to-task switches (i.e., rest to reward, rest to perception, and rest to working memory) in the current study.

Module partition similarity is the architectural similarity between resting partition and a task partition for a given module. High similarity indicates stable module architecture and thus low flexibility. The same community detection procedure used for whole-brain architecture was performed for each state and each module.

To examine the potential age effects in the child sample, we examined the relationship between participants' age (in months) and the network measures. All significant p values survived correction for multiple comparisons using false discovery rate (Benjamini and Hochberg, 1995) unless otherwise noted.

3. Results

3.1. Global network architecture in different cognitive states

Using Louvain community detection algorithm, we characterized the whole-brain network architecture by identifying 12 functional network modules for each of the four cognitive states (i.e., resting, reward, perception, and working memory). The 12 communities were similar to those defined in adults (Power et al., 2011): somatomotor,

cingulo-opercular, auditory, default-mode, visual, frontoparietal, salience, subcortical, ventral attention, dorsal attention, and cerebellum. The optimal resting-state community detection parameters were then applied to the three task states, similarly yielding 12 communities for each task (Fig. 2A). Partition similarity was higher among the three task states than between resting and task states (p 's < 0.01) (Fig. 2B). Reward-resting partition similarity was significantly greater than perception-resting partition similarity ($t(51) = 2.43, p = .018$) but only marginally greater than working memory-resting partition similarity ($p = .17$). Partition similarity did not exhibit a significant relationship with differences in amount of data (in scan volume) between states (p 's > .12).

To determine whether the child sample's rsFC network architecture was comparable to that in adults, we measured partition similarity between our 60-child sample of usable resting state data, a subset of 60 adults in the CB resting-state dataset, and the published adult network architecture (Power et al., 2011). As expected, while the resting network architecture of our child sample showed high similarity to the adult network architecture defined by Power et al. (M [SD] = .25 [.06]), the degree of similarity was significantly higher between the two adult samples (i.e., CB and Power et al. network architectures) (M [SD] = .29 [.05]) ($t(118) = 3.8, p < .001$). Further, we found an age effect in our child sample such that the degree of partition similarity between the CB average network partition and each children's network partition was positively correlated with the children's age (in months) ($r = .33, p = .01$) (Fig. 2C). To rule out potential confounding effects of head motion, we performed the same regression analysis while controlling for the mean and median DVARS and FD in each run and found the resulting age effect remained significant ($r = .34, p = .016$).

We further examined whether the degree of similarity in rsFC network architecture between the child and CB samples varied across the functional network modules. The child sample's Salience (M [SD] = .14 [.11]) and FPN (M [SD] = .15 [.1]) modules were significantly less

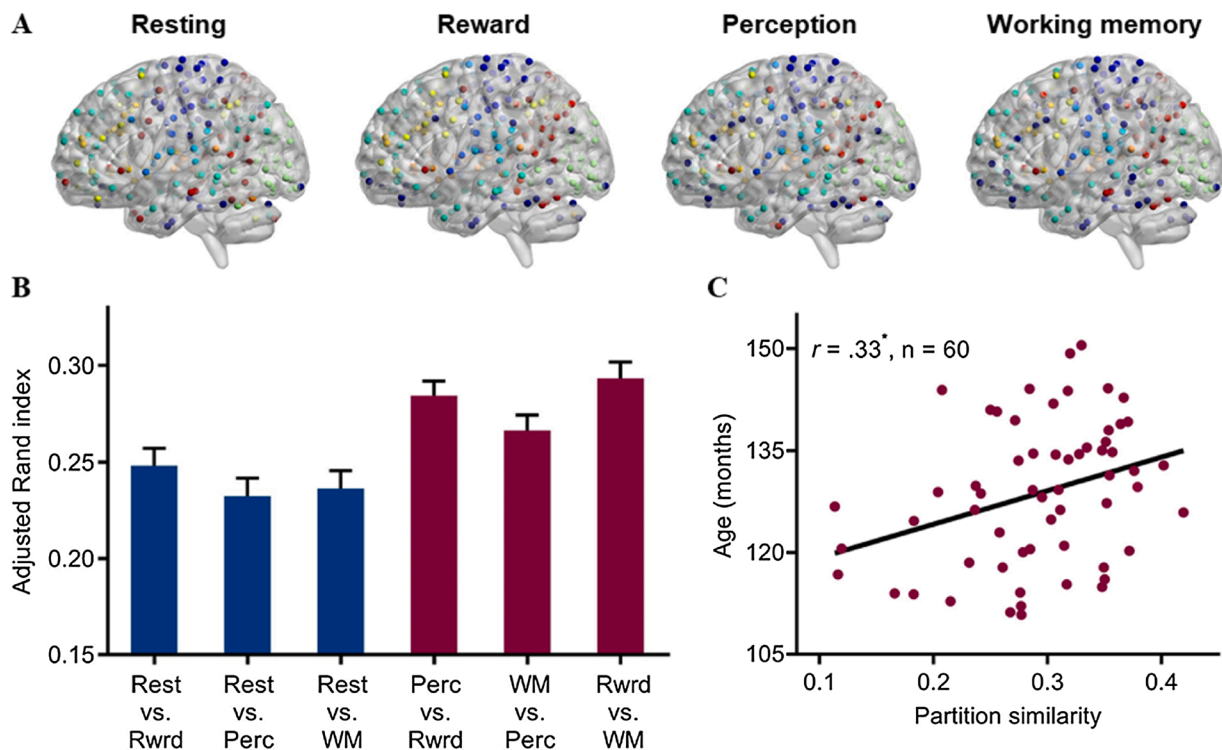


Fig. 2. Whole-brain network architecture in each state. (A) Louvain community detection algorithm was used to identify 12 communities (in different colors) in resting, reward task, perception task, and working memory task. (B) Adjusted Rand index of partition similarity was higher among the three task states than between resting and task states. (C) Partition similarity of whole-brain resting-state network between children and young adults was positively correlated with the children's age. * $p \leq .01$.

similar to the CB sample than the other modules (all p 's < .001), whereas the DMN (M [SD] = .19 [.06]), Visual (M [SD] = .2 [.08]) and SMN (M [SD] = .23 [.1]) were more similar.

In sum, children in early adolescence showed stable whole-brain network architecture across various cognitive states but with detectable differences between resting and task states. The degree of similarity to the adult network architecture at rest varied with age and network modules.

3.2. Functional integration and flexibility across cognitive state

Next, we examined functional integration in the 52 children with usable data from the resting and three task states. Greater whole-brain network integration was found for all task states relative to the resting state. Specifically, the task states exhibited significant increases in global efficiency, number of connector hubs, and participation coefficient compared to the resting state (p 's < .002) (Fig. 3A-C).

There was a significant decrease in local efficiency from the resting to task states (corrected p 's < .001) (Fig. 3D). However, modularity did not significantly differ across the four states (p 's > .28) (Fig. 3E). As reduced modularity was associated with increased cognitive processing in adults (Cohen and D'Esposito, 2016), we examined the effect of age on modularity and found that the older the participants, the lower the degree of modularity in task state (averaged across the three tasks) ($r = -.35$, $p = .01$) (Fig. 3F). It is worth noting that most integration measures during the resting state were comparable to the CB adult sample (p 's > .14), with the exception of participation coefficient which was higher in the child sample ($t(110) = 4.13$, $p < .001$).

To rule out the potential confounding effects of head motion, we confirmed that there were no significant correlations between the mean/median FD/DVARS and each network integration measure across the children (p 's > .19). FD was found to be significantly higher for task states (working memory = $.19 \pm .08$, reward = $.18 \pm .09$, perception = $.17 \pm .08$, $M \pm SD$) relative to resting state ($.14 \pm .07$) (p 's $\leq .029$). 3 subjects showed significantly greater FD than the group (i.e., beyond 3 SD from the mean), one in each of resting, working memory, and

perception run. The removal of these subjects did not significantly alter any of the findings of network integration.

To examine functional flexibility, we used the DMN, FPN, Salience, Visual, and SMN functional modules identified in the resting state (Fig. 4A) and extracted connectivity variability, nodal membership change, and partition similarity across the four states for each network.

Among the networks, FPN showed the higher variability in connectivity strength across states than DMN ($p = .004$), visual network ($p < .001$), SMN ($p < .001$), and Salience network ($p < .001$) (Fig. 4B) whereas variability was lowest in the visual network (p 's < .001). Similarly, FPN showed the highest nodal membership change (p 's $\leq .001$) (Fig. 4C). Note that all comparisons were significant after correction for multiple comparisons. In addition, relative to all other modules, FPN and Salience showed lowest rest-task partition similarity (p 's < .05), indicating a higher degree of architectural changes (Fig. 4D). In sum, FPN (and to a lesser degree, Salience) showed greatest functional flexibility whereas sensory and motor modules exhibited relatively more stable connectivity patterns across the four states.

Finally, we conducted additional analyses to examine to what extent these network integration observations may have been confounded by small head motions or motion differences between rest and task states. All global and modular effects maintained after removing the subjects with average FD > 0.3 mm ($N = 13$) or those that showed non-matching FD between states ($N = 15$), with the exception of the age and modularity association (respectively $r = -.39$, $p = .014$ and $r = -.22$, $p = .18$; compared with Fig. 3F).

3.3. Relationship between connectivity profiles and task performance

We conducted exploratory analysis to examine whether integration and flexibility in network properties were associated with individual differences in behavioral performance in the working memory and visual perception tasks. (We did not examine the reward task due to the lack of interpretable behavioral measures.)

For load effect on working memory performance (L3-L1Acc, accuracy difference between Load 3 and Load 1), there was a negative

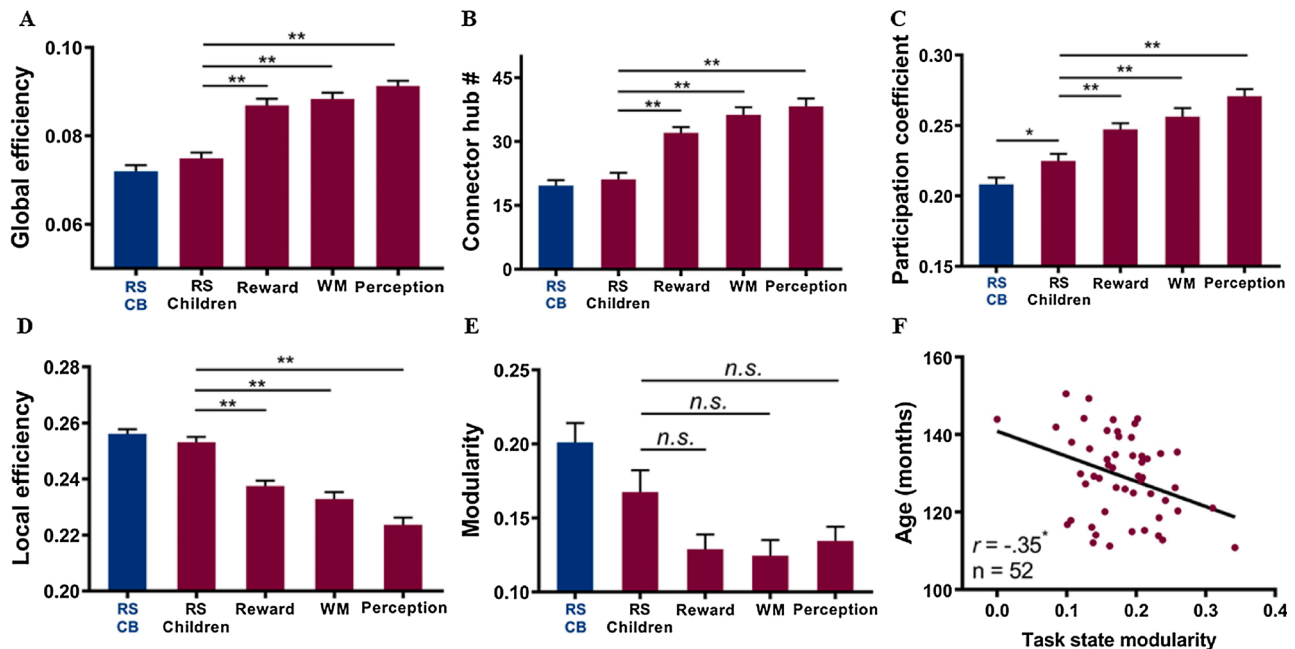


Fig. 3. Measures of whole-brain network integration during various task states: (A) global efficiency, (B) number of connector hubs, (C) participation coefficient, (D) local efficiency, and (E) modularity. There was a general increase in the degree of integration in task states relative to resting state, and a negative correlation between age and task-state modularity (F). For comparison, measures of integration during resting state were shown in the plots for the CB sample (blue bars). Abbreviation: CB – Cambridge Buckner, RS – resting state, WM – working memory. ** $p \leq .001$, * $p \leq .01$, *n.s.* not significant (For interpretation of the references to colour in this figure legend, the reader is referred to the web version of this article).

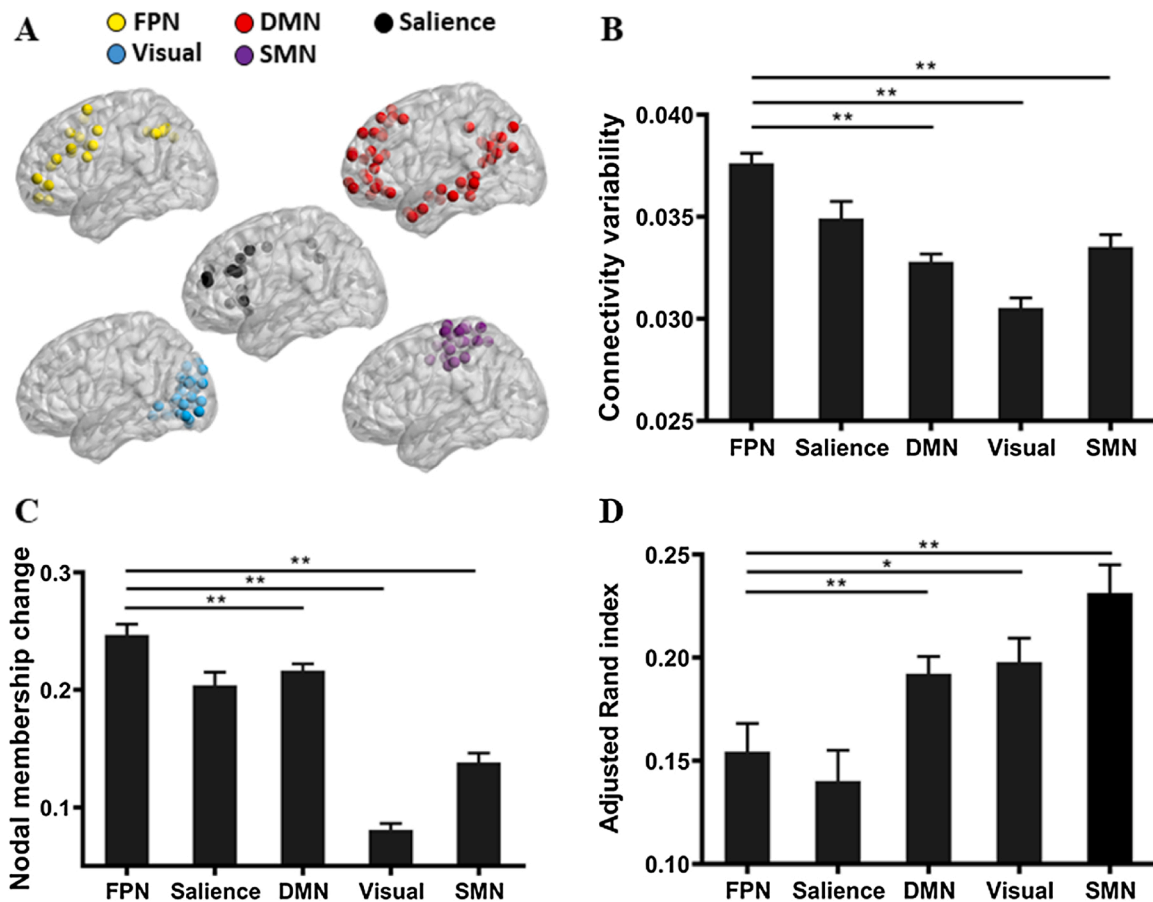


Fig. 4. Flexibility of the functional network modules across states. (A) Five network modules identified by community detection: FPN, DMN, Saliency, Visual, and Somatomotor. (B) Connectivity variability coefficient showed variability in connectivity strength measured by standard deviation across the four states. (C) Nodal membership change showed the probability of nodes switching their module membership when transitioning from resting to task states. (D) Partition similarity showed the similarity in module architecture between resting and task states. Abbreviation: DMN – default mode network, FPN – frontoparietal network, SMN – somatomotor network.

association between the number of connector hubs and the performance difference between working memory load ($r = .49, p = .003$) (Fig. 5A), suggesting that larger performance difference or larger load effect was related to a higher degree of inter-modular connectivity. In contrast, rest-WM partition similarity was positively associated with better L3-L1Acc ($r = -.41, p = .014$) (Fig. 5B), suggesting a less changes in community architecture is associated with more stable performance across working memory load.

For the perception task, global efficiency during visual perception was positively associated with performance accuracy ($r = .34, p = .037$, not significant after correction for multiple comparisons) (Fig. 5C). At the module level, average FPN, Saliency, DMN, Visual, and SMN partition similarity between resting and perception state was negatively correlated with performance accuracy ($r = -.41, p = .009$) (Fig. 5D). The relationship between performance accuracy and whole-brain partition similarity was not significant ($p = .13$). Taken together, these results suggest a low degree of network integration and flexibility is beneficial to working memory performance, whereas more flexibility in network connectivity is beneficial to perceptual performance.

4. Discussion

We found that functional brain networks in children during late childhood and early adolescence exhibited age- and state-dependent connectivity patterns while showing broad adult-like organization. Specifically, during resting, the whole-brain network was organized into distinct modules as previously identified in adults (Power et al., 2011).

During task states, the connectivity at the whole-brain level became more integrated as reported in adults (Cohen and D'Esposito, 2016). At the module level, networks implicated in executive function or multi-modal processing exhibited highly variable connectivity patterns across task states involving working memory, decision making, and visual perception whereas those associated with motor and sensory processing remained relatively stable. Such results are consistent with previous work suggesting the emergence of core neurocognitive networks in the development of cognitive abilities (Casey et al., 2005). Age-related characteristics were found in task-induced modularity as well as in the intrinsic network architecture upon comparison with a sample of young adults. Thus, the functional brain in late childhood and early adolescence demonstrates network properties that reflected both cognitive demands and the continuing neural maturation.

4.1. Functional network architecture in late childhood

The current study showed that the functional organization of the whole brain network during resting state fMRI in children aged 9–12 maps well with the same 12 core modules previously identified in adults (Power et al., 2011). Also consistent with the adult literature (Cole et al., 2014), this architecture remained relatively preserved during the subsequent performance of cognitive tasks that involved working memory, rewarded decision making, and perception. Such finding adds to the growing literature characterizing the maturation of functional neural networks from infancy to adulthood. Between the age of 1 month to 2 years, the brain begins to form core rsFC networks such as the DMN and

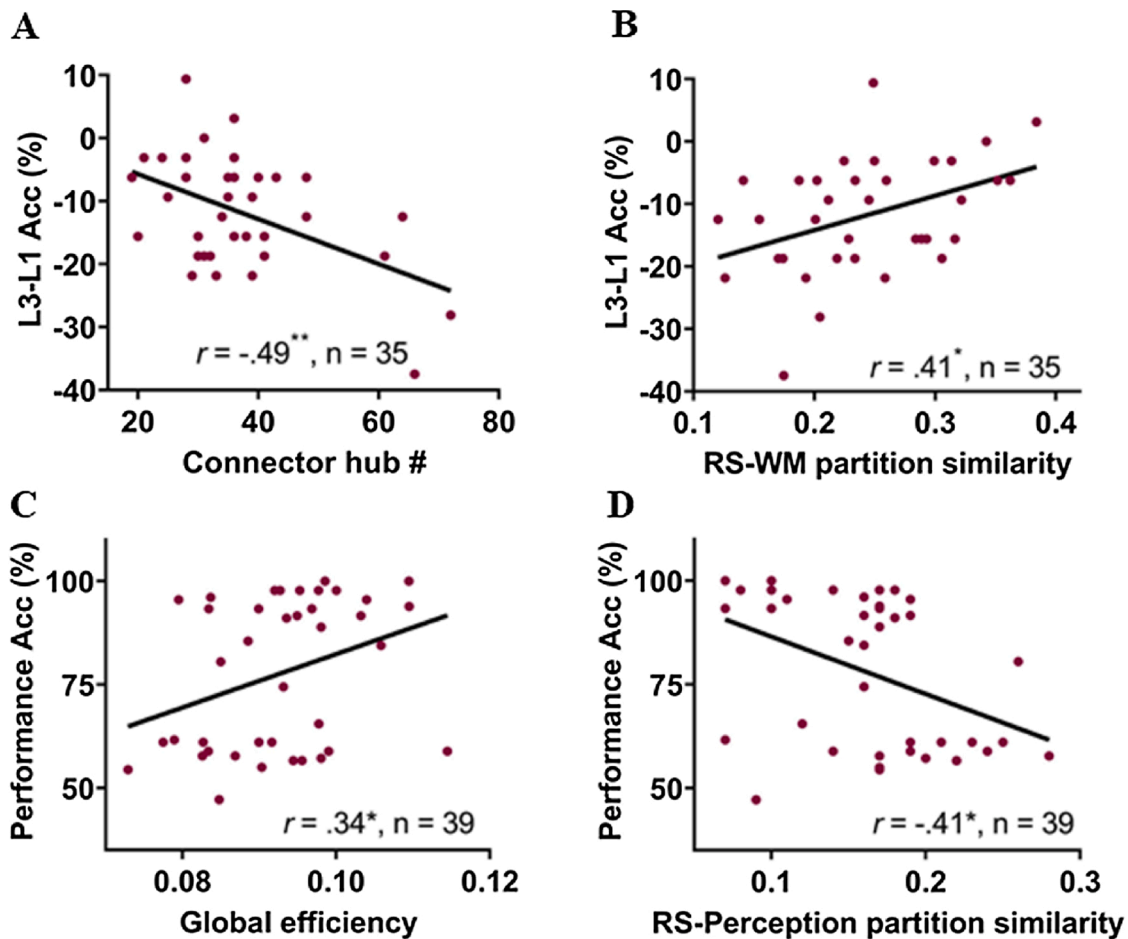


Fig. 5. Relationship between network properties and behavioral performance across children. For the working memory task, smaller load effect (closer to 0 in L3-L1 accuracy difference) was associated with the smaller number of connector hubs during the task state (A) and higher whole-brain partition similarity between resting and task state (i.e., less changes in network architecture) (B). For the perception task, better performance was associated with higher global efficiency during the task state (C) and lower partition similarity between resting and task states across the 5 functional modules (D). Abbreviation: Acc – accuracy, L1/3: working memory load 1/3, RS – resting state, WM – working memory. * $p < .05$, ** $p < .01$.

dorsal attention network (Gao et al., 2013; Lee et al., 2013) and exhibits progressively modular organization and efficient connectivity patterns (Fan et al., 2011). By age 7, the intrinsic whole-brain network architecture in children is comparable to that in adults, as reflected by similarity in measures including path length, clustering coefficient, small-worldness, and global efficiency between the two age groups (Cao et al., 2017). Nevertheless, a recent diffusion tensor imaging study found that the structural brain networks continue to show greater segregation and efficiency between the age of 8 and 22 (Baum et al., 2017), suggesting ongoing structural changes from late childhood into early adulthood.

Our findings show complementary functional evidence of age-dependent functional network organization in late childhood and early adolescence. At the whole-brain level, we observed significantly lower architectural similarity between the child and CB samples than that between the two adult groups and a positive correlation between the children's age and architectural similarity to the CB sample. At the module level, FPN was the least similar to that in adults while visual and motor modules were the most similar, indicating different maturation trajectories for different networks. While reorganization of association and sensory cortical functional connectivity is recently reported in post-adolescence (Váša et al., 2020), our findings are in agreement with both rsFC (de Bie et al., 2012) and morphometric (Gogtay et al., 2004; Lenroot and Giedd, 2006; Shaw et al., 2008) evidence of the protracted maturation of the frontal lobe relative to visual and motor cortices. More specifically, during adolescence, the frontal regions have been found to

show accelerated gray matter density loss, indicating synaptic pruning, later than brain structures supporting visuospatial functions (Sowell et al., 2001, 1999). Such findings are in line with behavioral observations of early development of sensory capacity relative to executive functions (Simmering, 2012; Weil et al., 2013). Thus, although the functional intrinsic network architecture is well defined by late childhood, it likely continues to refine in the years toward adulthood.

Another adult-like characteristic of the intrinsic whole-brain network in children is its preservation of the 12-community architecture across the working memory, reward, and perception tasks. Previous investigations have found minimal changes in network organization across multiple cognitive tasks in adults (Cole et al., 2014; Krienen et al., 2014). Our findings thus suggest that fundamental functional network architecture underlying both resting and complex cognitive states also exists in children. The presence of such intrinsic architecture may reflect constraints from anatomical connections (Krienen et al., 2014). It is also possible that the stability of network configurations may have been partially attributable to the acquisition of all task data in a single scan session (Krienen et al., 2014). Nevertheless, previous research showed moderate to high test-retest reliability in rsFC connectivity patterns including network clustering in 3 scans acquired at least 5 months apart (Shehzad et al., 2009), indicating stable network organization over time.

4.2. Shift toward global functional integration during cognitive processing

While the intrinsic functional networks in children showed both

adult-like and age-related characteristics, it was unclear whether they respond to cognitive demands in manners similar to those previously observed in adults. One well-replicated finding in the literature is the enhanced integration in network connectivity during cognitively demanding tasks such as working memory, decision making, attention, and rule learning relative to rest (Cohen and D'Esposito, 2016; Cole et al., 2013; Davison et al., 2015; Shine et al., 2016). Indeed, we found that most measures of integration including global efficiency, connector hubs, and participation coefficient were significantly higher during task states than resting in our child sample. Functional integration is proposed to reflect the convergence and joint processing of specialized information across distributed circuits collectively involved in task completion (Sporns, 2013). In support, visual working memory has been shown to involve enhanced connectivity among distributed regions including visual association, parietal, frontal, and subcortical areas (Gazzaley et al., 2004). Similarly, face perception engages connectivity not only in core visual regions (e.g., fusiform gyrus) but also regions implicated in control and valence processing such as the amygdala, orbitofrontal cortex, and inferior frontal gyrus (Fairhall and Ishai, 2007). These findings corroborate the notion that transient and flexible increases in distributed cortical coordination are necessary for effortful cognitive processing (Bressler and Kelso, 2001; Fries, 2005). In the developmental literature, widespread brain activations were observed in children, likely reflecting involvement from multiple brain networks in tasks including working memory (Güler and Thomas, 2013; O'Hare et al., 2008), tracking stop (Rubia et al., 2007), go/no-go (Mostofsky et al., 2007), and flanker (Zalecki et al., 2005). Nevertheless, to the best of our knowledge, our study is the first to provide evidence that the child brain exhibits task-induced integration across large scale functional networks.

While the brain during late childhood and early adolescence demonstrated enhanced integration by most measures following increased cognitive demand, we found the lack of modularity reduction, seemingly inconsistent with the adult literature (Cao et al., 2014; Cohen and D'Esposito, 2016). Modularity, a crucial feature of complex neural systems (Sporns and Betzel, 2016), is observed early in development and increasing with age as shown in structural (Fan et al., 2011) and rsFC (Betzel et al., 2014) investigations. However, the degree of modularity continue to change between adolescence and adulthood, as demonstrated by the sparser long-range connections but denser short-range connections during this stage of development (Betzel et al., 2014; Stevens, 2016). Such differences likely impact the functional brain properties during cognitive processing. Indeed, we found a negative association between task-state modularity and participants' age, suggesting that task-evoked modularity may represent a marker for brain maturation. Taken together, the child brain shows the capability to shift toward functional integration in response to cognitive demand but this shift is still constrained by the ongoing fine-tuning process during neural circuitry maturation.

4.3. Executive control, visual, and motor networks show different patterns of flexibility

A notable characteristic of the complex functional neural system is its flexibility in reorganizing connectivity patterns in response to changing cognitive demands (Bassett et al., 2015b, 2010). It has been suggested that flexibility may represent an indirect measurement of the transitions between cognitive processes (Braun et al., 2015; Deco et al., 2009; McIntosh et al., 2008). In late childhood, we found that the brain also exhibited a high degree of variability in network architecture, nodal membership switches, and connectivity strength, especially in modules associated with executive control including the frontoparietal and salience networks. A similar finding was previously reported in adults who showed greatest connectivity variability in the FPN, compared with other networks, during the performance of a variety of tasks (Cole et al., 2013). The variability in FPN connectivity may have been related to the

coding of distinct information associated with different cognitive states (Cole et al., 2013). In a study of visuomotor learning, connectivity patterns in the motor and visual networks changed little over time whereas multimodal association regions exhibited significantly greater flexibility (Bassett et al., 2013). High FPN variability may be related to the network's recruitment across diverse cognitive domains (Crittenden et al., 2016; Niendam et al., 2012) and involvement in the processing (Duncan, 2010) and switching (Kim et al., 2012) of sequential task information. Reports from non-human primate research further corroborates the FPN flexibility account. Different cognitive demands have been associated with different activity patterns of prefrontal neurons as demonstrated by electrophysiological recordings in monkeys performing a cue-target association task (Sigala et al., 2008). The transitions between tasks elicited changes not only in cellular firing rates but also in patterns of correlation between cells of the frontal cortex (Tishby et al., 1999; Vaadia et al., 1995).

Our findings expand on previous research by showing that variability in network connectivity across task states is present in early childhood despite the slow maturation rate of the FPN. For example, variability of the neurocognitive network rsFC has been shown in positive correlation with age in children between age 7 and 16 (Marusak et al., 2017). Variability in multiscale entropy of EEG and MEG signals during visual perception in various brain regions including the visual and parietal cortices was also found to increase with age starting from infancy and early childhood (Lippe et al., 2009) to adolescence (McIntosh et al., 2008) and adulthood (Mišić et al., 2010). As neural flexibility has been associated with intelligence and executive function in adults (Duncan, 2010; Nomi et al., 2017), evidence of the FPN's flexibility in connectivity patterns across tasks may offer implications for cognitive development in children. The ability to switch between different cognitive demands is of particular relevance in late childhood/early adolescence as this skill (Dick, 2014), along with executive function (Anderson, 2002), undergoes a sharp increase in proficiency during this stage. Such milestone in cognitive development coincides with the frontal and parietal gray matter reaching maximal volume (Giedd et al., 1999). These findings indicate a possible relationship between structural and functional maturation of the FPN and the development of cognitive flexibility in this age group.

4.4. Relationship between behavioral performance and functional network connectivity patterns

Our exploratory analysis showed a potential relationship between behavioral performance and the degree of functional integration and flexibility. In the perception task, better performance was associated with greater global efficiency and dissimilarity between resting-task architecture, suggesting perceptual performance may benefit from a connectivity profile of enhanced network integration and flexible connectivity. Previous work in young adults showed widespread activation (Oh and Leung, 2009) and connectivity (Le et al., 2017) involving temporo-occipital and frontoparietal systems during the processing of face and scene information. In children, while the fine-tuning of neural selectivity continue to occur into adolescence (Cohen Kadosh and Johnson, 2007), similar activation patterns during face and scene perception (Scherf et al., 2007) have been observed. Thus, integration and flexible functional connectivity may better support processing of new sensory information and respond to constant changes in the sensory environment (Irwin and Wynn, 2015; Prime et al., 2011).

In the working memory task, the connectivity profile suggests some degree of functional segregation and stability may have helped behavioral performance or reduce load effect. This finding seemingly differs from a previous report showing a relationship between enhanced working memory performance and increased functional integration in healthy adults (Cohen and D'Esposito, 2016). However, while modularity decreases in adults during cognitively demanding tasks (Cohen and D'Esposito, 2016; Liang et al., 2016), the measure was not

significantly lower during task states in our child sample. Past research has indicated stable activation during working memory may be beneficial (Hampson et al., 2006; Otten and Rugg, 2001) whereas abnormally high variability during working memory can be detrimental to performance as shown in the case of distractors (Armbruster-Genc et al., 2016) or individuals with schizophrenia (Manoach, 2003; Meyer-Lindenberg et al., 2001). During working memory, relevant information may benefit from protection against interference (Jonides and Nee, 2006; Kane and Engle, 2000; Le et al., 2017; Lustig et al., 2001). Thus, it is plausible that a moderate degree of flexibility and modularity may have been advantageous in the current sample.

5. Limitations and conclusions

As our child participants were recruited from a community population with and without parental history of depression, hereditary factors associated with the disorder may have influenced neural network configuration changes across states. Previous research has indeed found depression-specific alterations in functional connectivity (Connolly et al., 2013; Zeng et al., 2012). However, we used measures of negative and positive emotionality collected from our child sample and found no significant relationship between these measures and the network indices (data not shown). Nevertheless, the potential effects of family history of mood disorders on functional network architecture in children remain unknown and thus require further research.

In sum, the current study shows that the intrinsic neural network architecture in late childhood and early adolescence is similar to that in young adults. The degree of similarity was closely related to age, indicating the fine-tuning of the network architecture during this stage of development. During various task states, although the network architecture largely retained its basic configuration as previously shown in adults, network connectivity patterns exhibited greater integration with increased cognitive demand. At the module level, the FPN and SN were more flexible and variable whereas the sensory and motor modules remained relatively stable across the task states. These findings add to the understanding of the spatiotemporal patterns of cortical network organization in the youth brain during various cognitive states and how they may help explain brain, cognitive, and behavioral development.

Funding source

Stony Brook Research Foundation (Leung).

Declaration of Competing Interest

The authors declare no conflict of interest.

Acknowledgements

We are grateful to Dr. Daniel Klein for the generous support in data collection and access to the participants. We also thank Kim Burke and staff of the SCAN center for their technical support during image acquisition.

References

- Anderson, P., 2002. Assessment and development of executive function (EF) during childhood. *Child Neuropsychol.* 8, 71–82. <https://doi.org/10.1076/chin.8.2.71.8724>.
- Arabic, P., Hubert, L., 1985. Comparing partitions. *J. Classif.* 2, 193–218. <https://doi.org/10.1007/BF01908075>.
- Armbruster-Genc, D.J.N., Ueltzhoffer, K., Fiebach, C.J., 2016. Brain signal variability differentially affects cognitive flexibility and cognitive stability. *J. Neurosci.* 36, 3978–3987. <https://doi.org/10.1523/JNEUROSCI.2517-14.2016>.
- Baker, S.T.E., Lubman, D.I., Yucel, M., Allen, N.B., Whittle, S., Fulcher, B.D., Zalesky, A., Fornito, A., 2015. Developmental changes in brain network hub connectivity in late adolescence. *J. Neurosci.* 35, 9078–9087. <https://doi.org/10.1523/jneurosci.5043-14.2015>.

- Bassett, D.S., Gazzaniga, M.S., 2011. Understanding complexity in the human brain. *Trends Cogn. Sci.* 15, 200–209. <https://doi.org/10.1016/j.tics.2011.03.006>.
- Bassett, D.S., Wymbs, N.F., Porter, M.A., Mucha, P.J., Carlson, J.M., Grafton, S.T., 2010. Dynamic reconfiguration of human brain networks during learning. *Proc. Natl. Acad. Sci.* 108, 7641–7646. <https://doi.org/10.1073/pnas.1018985108>.
- Bassett, D.S., Wymbs, N.F., Rombach, M.P., Porter, M.A., Mucha, P.J., Grafton, S.T., 2013. Task-based core-periphery organization of human brain dynamics. *PLoS Comput. Biol.* 9, 1–16. <https://doi.org/10.1371/journal.pcbi.1003171>.
- Bassett, D.S., Yang, M., Wymbs, N.F., Grafton, S.T., 2015a. Learning-induced autonomy of sensorimotor systems. *Nat. Neurosci.* 18, 744–751. <https://doi.org/10.1038/nn.3993>.
- Bassett, D.S., Yang, M., Wymbs, N.F., Grafton, S.T., 2015b. Learning-induced autonomy of sensorimotor systems. *Nat. Neurosci.* 18, 744–751. <https://doi.org/10.1038/nn.3993>.
- Baum, G.L., Ciric, R., Roalf, D.R., Betzel, R.F., Moore, T.M., Shinohara, R.T., Kahn, A.E., Vandekar, S.N., Rupert, P.E., Quarmley, M., Cook, P.A., Elliott, M.A., Ruparel, K., Gur, R.E., Gur, R.C., Bassett, D.S., Satterthwaite, T.D., 2017. Modular segregation of structural brain networks supports the development of executive function in youth. *Curr. Biol.* 27, 1561–1572.e8. <https://doi.org/10.1016/j.cub.2017.04.051>.
- Behzadi, Y., Restom, K., Liaw, J., Liu, T.T., 2007. A component based noise correction method (CompCor) for BOLD and perfusion based fMRI. *Neuroimage* 37, 90–101. <https://doi.org/10.1016/j.neuroimage.2007.04.042>.
- Benjamini, Y., Hochberg, Y., 1995. Controlling the false discovery rate: a practical and powerful approach to multiple testing. *J. R. Stat. Soc. Ser. B* 57, 289–300. <https://doi.org/10.1111/j.2517-6161.1995.tb02031.x>.
- Betzel, R.F., Byrge, L., He, Y., Goñi, J., Zuo, X.N., Sporns, O., 2014. Changes in structural and functional connectivity among resting-state networks across the human lifespan. *Neuroimage* 102, 345–357. <https://doi.org/10.1016/j.neuroimage.2014.07.067>.
- Biswal, B.B., Mennes, M., Zuo, X.-N., Gohel, S., Kelly, C., Smith, S.M., Beckmann, C.F., Adelman, J.S., Buckner, R.L., Colcombe, S., Dagonowski, A.-M., Ernst, M., Fair, D., Hampson, M., Hoptman, M.J., Hyde, J.S., Kiviniemi, V.J., Kötter, R., Li, S.-J., Lin, C.-P., Lowe, M.J., Mackay, C., Madden, D.J., Madsen, K.H., Margulies, D.S., Mayberg, H.S., McMahon, K., Monk, C.S., Mostofsky, S.H., Nagel, B.J., Pekar, J.J., Peltier, S.J., Petersen, S.E., Riedel, V., Rombouts, S.A.R.B., Rypma, B., Schlaggar, B.L., Schmidt, S., Seidler, R.D., Siegle, G.J., Sorg, C., Teng, G.-J., Veijola, J., Villringer, A., Walter, M., Wang, L., Weng, X.-C., Whitfield-Gabrieli, S., Williamson, P., Windischberger, C., Zang, Y.-F., Zhang, H.-Y., Castellanos, F.X., Milham, M.P., 2010. Toward discovery science of human brain function. *Proc. Natl. Acad. Sci.* 107, 4734–4739. <https://doi.org/10.1073/pnas.0911855107>.
- Braun, U., Schäfer, A., Walter, H., Erk, S., Romanczuk-Seiferth, N., Haddad, L., Schweiger, J.L., Grimm, O., Heinz, A., Tost, H., Meyer-Lindenberg, A., Bassett, D.S., 2015. Dynamic reconfiguration of frontal brain networks during executive cognition in humans. *Proc. Natl. Acad. Sci. U. S. A.* 112, 11678–11683. <https://doi.org/10.1073/pnas.1422487112>.
- Bressler, S.L., Kelso, J.A.S., 2001. Cortical coordination dynamics and cognition. *Trends Cogn. Sci.* 5, 26–36. [https://doi.org/10.1016/S1364-6613\(00\)01564-3](https://doi.org/10.1016/S1364-6613(00)01564-3).
- Cao, H., Plichta, M.M., Schäfer, A., Haddad, L., Grimm, O., Schneider, M., Esslinger, C., Kirsch, P., Meyer-Lindenberg, A., Tost, H., 2014. Test-retest reliability of fMRI-based graph theoretical properties during working memory, emotion processing, and resting state. *Neuroimage* 84, 888–900. <https://doi.org/10.1016/j.neuroimage.2013.09.013>.
- Cao, M., Huang, H., He, Y., 2017. Developmental connectomics from infancy through early childhood. *Trends Neurosci.* 40, 494–506. <https://doi.org/10.1016/j.tins.2017.06.003>.
- Casey, B.J., Galvan, A., Hare, T.A., 2005. Changes in cerebral functional organization during cognitive development. *Curr. Opin. Neurobiol.* 15, 239–244. <https://doi.org/10.1016/j.conb.2005.03.012>.
- Chevalier, N., Blaye, A., 2009. Setting goals to switch between tasks: effect of cue transparency on children's cognitive flexibility. *Dev. Psychol.* 45, 782–797. <https://doi.org/10.1037/a0015409>.
- Cohen, J.R., D'Esposito, M., 2016. The segregation and integration of distinct brain networks and their relationship to cognition. *J. Neurosci.* 36, 12083–12094. <https://doi.org/10.1523/JNEUROSCI.2965-15.2016>.
- Cohen Kadosh, K., Johnson, M.H., 2007. Developing a cortex specialized for face perception. *Trends Cogn. Sci.* 11, 367–369. <https://doi.org/10.1016/j.tics.2007.06.007>.
- Cole, M.W., Reynolds, J.R., Power, J.D., Repovs, G., Anticevic, A., Braver, T.S., 2013. Multi-task connectivity reveals flexible hubs for adaptive task control. *Nat. Neurosci.* 16, 1348–1355. <https://doi.org/10.1038/nn.3470>.
- Cole, M.W., Bassett, D.S., Power, J.D., Braver, T.S., Petersen, S.E., 2014. Intrinsic and task-evoked network architectures of the human brain. *Neuron* 83, 238–251. <https://doi.org/10.1016/j.neuron.2014.05.014>.
- Connolly, C.G., Wu, J., Ho, T.C., Hoefl, F., Wolkowitz, O., Eisendrath, S., Frank, G., Hendren, R., Max, J.E., Paulus, M.P., Tapert, S.F., Banerjee, D., Simmons, A.N., Yang, T.T., 2013. Resting-state functional connectivity of subgenual anterior cingulate cortex in depressed adolescents. *Biol. Psychiatry* 74, 898–907. <https://doi.org/10.1016/j.biopsych.2013.05.036>.
- Crittenden, B.M., Mitchell, D.J., Duncan, J., 2016. Task encoding across the multiple demand cortex is consistent with a frontoparietal and cingulo-opercular dual networks distinction. *J. Neurosci.* 36, 6147–6155. <https://doi.org/10.1523/JNEUROSCI.4590-15.2016>.
- Dajani, D.R., Uddin, L.Q., 2015. Demystifying cognitive flexibility: implications for clinical and developmental neuroscience. *Trends Neurosci.* 38, 571–578. <https://doi.org/10.1016/j.tins.2015.07.003>.
- Davidson, M.C., Amso, D., Anderson, L.C., Diamond, A., 2006. Development of cognitive control and executive functions from 4 to 13 years: evidence from manipulations of

- memory, inhibition, and task switching. *Neuropsychologia* 44, 2037–2078. <https://doi.org/10.1016/j.neuropsychologia.2006.02.006>.
- Davison, E.N., Schlesinger, K.J., Bassett, D.S., Lynall, M.E., Miller, M.B., Grafton, S.T., Carlson, J.M., 2015. Brain network adaptability across task states. *PLoS Comput. Biol.* 11, e1004029 <https://doi.org/10.1371/journal.pcbi.1004029>.
- de Bie, H.M.A., Boersma, M., Adriaanse, S., Veltman, D.J., Wink, A.M., Roosendaal, S.D., Barkhof, F., Stam, C.J., Oostrom, K.J., Delemarre-van de Waal, H.A., Sanz-Arigita, E. J., 2012. Resting-state networks in awake five- to eight-year old children. *Hum. Brain Mapp.* 33, 1189–1201. <https://doi.org/10.1002/hbm.21280>.
- Deco, G., Rolls, E.T., Romo, R., 2009. Stochastic dynamics as a principle of brain function. *Prog. Neurobiol.* 88, 1–16. <https://doi.org/10.1016/j.pneurobio.2009.01.006>.
- Dick, A.S., 2014. The development of cognitive flexibility beyond the preschool period: an investigation using a modified Flexible Item Selection Task. *J. Exp. Child Psychol.* 125, 13–34. <https://doi.org/10.1016/j.jecp.2014.01.021>.
- Duncan, J., 2010. The multiple-demand (MD) system of the primate brain: mental programs for intelligent behaviour. *Trends Cogn. Sci.* 14, 172–179. <https://doi.org/10.1016/j.tics.2010.01.004>.
- Fairhall, S.L., Ishai, A., 2007. Effective connectivity within the distributed cortical network for face perception. *Cereb. Cortex* 17, 2400–2406. <https://doi.org/10.1093/cercor/bhl148>.
- Fan, Y., Shi, F., Smith, J.K., Lin, W., Gilmore, J.H., Shen, D., 2011. Brain anatomical networks in early human brain development. *Neuroimage* 54, 1862–1871. <https://doi.org/10.1016/j.neuroimage.2010.07.025>.
- Fries, P., 2005. A mechanism for cognitive dynamics: neuronal communication through neuronal coherence. *Trends Cogn. Sci.* 9, 474–480. <https://doi.org/10.1016/j.tics.2005.08.011>.
- Gao, W., Zhu, H., Giovanello, K.S., Smith, J.K., Shen, D., Gilmore, J.H., Lin, W., 2009. Evidence on the emergence of the brain's default network from 2-week-old to 2-year-old healthy pediatric subjects. *Proc. Natl. Acad. Sci.* 106, 6790–6795. <https://doi.org/10.1073/pnas.0811221106>.
- Gao, W., Gilmore, J.H., Shen, D., Smith, J.K., Zhu, H., Lin, W., 2013. The synchronization within and interaction between the default and dorsal attention networks in early infancy. *Cereb. Cortex* 23, 594–603. <https://doi.org/10.1093/cercor/bhs043>.
- Garrett, D.D., Kovacevic, N., McIntosh, A.R., Grady, C.L., 2013. The modulation of BOLD variability between cognitive states varies by age and processing speed. *Cereb. Cortex* 23, 684–693. <https://doi.org/10.1093/cercor/bhs055>.
- Gazzaley, A., Rissman, J., D'Esposito, M., 2004. Functional connectivity during working memory maintenance. *Cogn. Affect. Behav. Neurosci.* 4, 580–599. <https://doi.org/10.3758/CABN.4.4.580>.
- Giedd, J.N., Blumenthal, J., Jeffries, N.O., Castellanos, F.X., Liu, H., Zijdenbos, A., Paus, T., Evans, A.C., Rapoport, J.L., 1999. Brain development during childhood and adolescence: a longitudinal MRI study. *Nat. Neurosci.* 2, 861–863. <https://doi.org/10.1038/13158>.
- Gogtay, N., Giedd, J.N., Lusk, L., Hayashi, K.M., Greenstein, D., Vaituzis, A.C., Nugent, T. F., Herman, D.H., Clasen, L.S., Toga, A.W., Rapoport, J.L., Thompson, P.M., 2004. Dynamic mapping of human cortical development during childhood through early adulthood. *Proc. Natl. Acad. Sci. U. S. A.* 101, 8174–8179. <https://doi.org/10.1073/pnas.0402680101>.
- Grayson, D.S., Ray, S., Carpenter, S., Iyer, S., Dias, T.G.C., Stevens, C., Nigg, J.T., Fair, D. A., 2014. Structural and functional rich club organization of the brain in children and adults. *PLoS One* 9, 1–13. <https://doi.org/10.1371/journal.pone.0088297>.
- Guimera, R., Nunes Amaral, L.A., 2005a. Cartography of complex networks: modules and universal roles. *J. Stat. Mech. Theory Exp.* 2005, P02001 <https://doi.org/10.1088/1742-5468/2005/02/P02001>.
- Guimera, R., Nunes Amaral, L.A., 2005b. Functional cartography of complex metabolic networks. *Nature* 433, 895–900. <https://doi.org/10.1038/nature03288>.
- Güler, O.E., Thomas, K.M., 2013. Developmental differences in the neural correlates of relational encoding and recall in children: an event-related fMRI study. *Dev. Cogn. Neurosci.* 3, 106–116. <https://doi.org/10.1016/j.dcn.2012.07.001>.
- Hampson, M., Driesen, N.R., Skudlarski, P., Gore, J.C., Constable, R.T., 2006. Brain connectivity related to working memory performance. *J. Neurosci.* 26, 1338–1343. <https://doi.org/10.1523/JNEUROSCI.3408-06.2006>.
- Irwin, D.E., Wynn, K., 2015. Integrating eye movements information across saccadic. *Curr. Dir. Psychol. Sci.* 5, 94–100.
- Jonides, J., Nee, D.E., 2006. Brain mechanisms of proactive interference in working memory. *Neuroscience* 139, 181–193. <https://doi.org/10.1016/j.neuroscience.2005.06.042>.
- Kane, M.J., Engle, R.W., 2000. Working-memory capacity, proactive interference, and divided attention: limits on long-term memory retrieval. *J. Exp. Psychol. Learn. Mem. Cogn.* 26, 336–358. <https://doi.org/10.1037/0278-7393.26.2.336>.
- Kim, C., Cilles, S.E., Johnson, N.F., Gold, B.T., 2012. Domain general and domain preferential brain regions associated with different types of task switching: a Meta-Analysis. *Hum. Brain Mapp.* 33, 130–142. <https://doi.org/10.1002/hbm.21199>.
- Koshino, H., Carpenter, P.A., Minschew, N.J., Cherkassky, V.L., Keller, T.A., Just, M.A., 2005. Functional connectivity in an fMRI working memory task in high-functioning autism. *Neuroimage* 24, 810–821. <https://doi.org/10.1016/j.neuroimage.2004.09.028>.
- Koyama, M.S., Di Martino, A., Zuo, X.-N., Kelly, C., Mennes, M., Jugtagir, D.R., Castellanos, F.X., Milham, M.P., 2011. Resting-state functional connectivity indexes reading competence in children and adults. *J. Neurosci.* 31, 8617–8624. <https://doi.org/10.1523/jneurosci.4865-10.2011>.
- Krienen, F.M., Thomas Yeo, B.T., Buckner, R.L., 2014. Reconfigurable task-dependent functional coupling modes cluster around a core functional architecture. *Philos. Trans. R. Soc. B Biol. Sci.* 369, 20130526– <https://doi.org/10.1098/rstb.2013.0526>.
- Kujawa, A., Hajcak, G., Torpey, D., Kim, J., Klein, D.N., 2012. Electrocardiac reactivity to emotional faces in young children and associations with maternal and paternal depression. *J. Child Psychol. Psychiatry Allied Discip.* 53, 207–215. <https://doi.org/10.1111/j.1469-7610.2011.02461.x>.
- Lancichinetti, A., Fortunato, S., Kertész, J., 2009. Detecting the overlapping and hierarchical community structure in complex networks. *New J. Phys.* 11 <https://doi.org/10.1088/1367-2630/11/3/033015>.
- Latora, V., Marchiori, M., 2001. Efficient behavior of small-world networks. *Phys. Rev. Lett.* 87, 198701 <https://doi.org/10.1103/PhysRevLett.87.198701>.
- Le, T.M., Borghi, J.A., Kujawa, A.J., Klein, D.N., Leung, H.-C., 2017. Alterations in visual cortical activation and connectivity with prefrontal cortex during working memory updating in major depressive disorder. *Neuroimage Clin.* 14 <https://doi.org/10.1016/j.nicl.2017.01.004>.
- Lee, W., Morgan, B.R., Shroff, M.M., Sled, J.G., Taylor, M.J., 2013. The development of regional functional connectivity in preterm infants into early childhood. *Neuroradiology* 55. <https://doi.org/10.1007/s00234-013-1232-z>.
- Lenroot, R.K., Giedd, J.N., 2006. Brain development in children and adolescents: insights from anatomical magnetic resonance imaging. *Neurosci. Biobehav. Rev.* 30, 718–729. <https://doi.org/10.1016/j.neubiorev.2006.06.001>.
- Li, Y., Hu, Y., Zhao, M., Wang, Y., Huang, J., Chen, F., 2013. The neural pathway underlying a numerical working memory task in abacus-trained children and associated functional connectivity in the resting brain. *Brain Res.* 1539, 24–33. <https://doi.org/10.1016/j.brainres.2013.09.030>.
- Liang, X., Zou, Q., He, Y., Yang, Y., 2016. Topologically reorganized connectivity architecture of default-mode, executive-control, and salience networks across working memory task loads. *Cereb. Cortex* 26, 1501–1511. <https://doi.org/10.1093/cercor/bhu316>.
- Lin, H.Y., Tseng, W.Y.I., Lai, M.C., Matsuo, K., Gau, S.S.F., 2015. Altered resting-state frontoparietal control network in children with attention-deficit/hyperactivity disorder. *J. Int. Neuropsychol. Soc.* 21, 271–284. <https://doi.org/10.1017/S135561771500020X>.
- Lippe, S., Kovacevic, N., McIntosh, A.R., 2009. Differential maturation of brain signal complexity in the human auditory and visual system. *Front. Hum. Neurosci.* 3, 48. <https://doi.org/10.3389/fnhum.09.048.2009>.
- Lustig, C., May, C.P., Hasher, L., 2001. Working memory span and the role of proactive interference. *J. Exp. Psychol. Gen.* 130, 199–207. <https://doi.org/10.1037/0096-3445.130.2.199>.
- Manoach, D.S., 2003. Prefrontal cortex dysfunction during working memory performance in schizophrenia: reconciling discrepant findings. *Schizophr. Res.* 60, 285–298. [https://doi.org/10.1016/S0920-9964\(02\)00294-3](https://doi.org/10.1016/S0920-9964(02)00294-3).
- Marusak, H.A., Calhoun, V.D., Brown, S., Crespo, L.M., Sala-Hamrick, K., Gotlib, I.H., Thomason, M.E., 2017. Dynamic functional connectivity of neurocognitive networks in children. *Hum. Brain Mapp.* 38, 97–108. <https://doi.org/10.1002/hbm.23346>.
- McIntosh, A.R., Kovacevic, N., Itier, R.J., 2008. Increased brain signal variability accompanies lower behavioral variability in development. *PLoS Comput. Biol.* 4 <https://doi.org/10.1371/journal.pcbi.1000106>.
- Meyer-Lindenberg, A., Polin, J.B., Kohn, P.D., Holt, J.L., Egan, M.F., Weinberger, D.R., Berman, K.F., 2001. Evidence for abnormal cortical functional connectivity during working memory in schizophrenia. *Am. J. Psychiatry* 158, 1809–1817. <https://doi.org/10.1176/appi.ajp.158.11.1809>.
- Mišić, B., Mills, T., Taylor, M.J., McIntosh, A.R., 2010. Brain noise is task dependent and region specific. *J. Neurophysiol.* 104, 2667–2676. <https://doi.org/10.1152/jn.00648.2010>.
- Miskovic, V., Ma, X., Chou, C.A., Fan, M., Owens, M., Sayama, H., Gibb, B.E., 2015. Developmental changes in spontaneous electrocortical activity and network organization from early to late childhood. *Neuroimage* 118, 237–247. <https://doi.org/10.1016/j.neuroimage.2015.06.013>.
- Mostofsky, S.H., Denckla, M.B., Blankner, J.G., Simmonds, D.J., Suskauer, S.J., Fotedar, S., Pekar, J.J., 2007. Functional magnetic resonance imaging evidence for abnormalities in response selection in attention deficit hyperactivity disorder: differences in activation associated with response inhibition but not habitual motor response. *J. Cogn. Neurosci.* 20, 478–493. <https://doi.org/10.1162/jocn.2008.20032>.
- Murphy, K., Birn, R.M., Handwerker, D.A., Jones, T.B., Bandettini, P.A., 2009. The impact of global signal regression on resting state correlations: Are anti-correlated networks introduced? *Neuroimage* 44, 893–905. <https://doi.org/10.1016/j.neuroimage.2008.09.036>.
- Niendam, T.A., Laird, A.R., Ray, K.L., Dean, Y.M., Glahn, D.C., Carter, C.S., 2012. Meta-analytic evidence for a superordinate cognitive control network subserving diverse executive functions. *Cogn. Affect. Behav. Neurosci.* 12, 241–268. <https://doi.org/10.3758/s13415-011-0083-5>.
- Nomi, J.S., Vij, S.G., Dajani, D.R., Steimke, R., Damaraju, E., Rachakonda, S., Calhoun, V. D., Uddin, L.Q., 2017. Chronotopic patterns and neural flexibility underlie executive function. *Neuroimage* 147, 861–871. <https://doi.org/10.1016/j.neuroimage.2016.10.026>.
- O'Hare, E.D., Lu, L.H., Houston, S.M., Bookheimer, S.Y., Sowell, E.R., 2008. Neurodevelopmental changes in verbal working memory load-dependency: an fMRI investigation. *Neuroimage* 42, 1678–1685. <https://doi.org/10.1016/j.neuroimage.2008.05.057>.
- Oh, H., Leung, H.-C., 2009. Specific and nonspecific neural activity during selective processing of visual representations in working memory. *J. Cogn. Neurosci.* 22, 1–15. <https://doi.org/10.1162/jocn.2009.21250>.
- Otten, L.J., Rugg, M.D., 2001. When more means less: neural activity related to unsuccessful memory encoding. *Curr. Biol.* 11, 1528–1530. [https://doi.org/10.1016/S0960-9822\(01\)00454-7](https://doi.org/10.1016/S0960-9822(01)00454-7).

- Power, J.D., Cohen, A.L., Nelson, S.M., Wig, G.S., Barnes, K.A., Church, J.A., Vogel, A.C., Laumann, T.O., Miezin, F.M., Schlaggar, B.L., Petersen, S.E., 2011. Functional network organization of the human brain. *Neuron* 72, 665–678. <https://doi.org/10.1016/j.neuron.2011.09.006>.
- Power, J.D., Barnes, K.A., Snyder, A.Z., Schlaggar, B.L., Petersen, S.E., 2012. Spurious but systematic correlations in functional connectivity MRI networks arise from subject motion. *Neuroimage* 59, 2142–2154. <https://doi.org/10.1016/j.neuroimage.2011.10.018>.
- Prime, S.L., Vesia, M., Crawford, J.D., 2011. Cortical mechanisms for trans-saccadic memory and integration of multiple object features. *Philos. Trans. R. Soc. B Biol. Sci.* 366, 540–553. <https://doi.org/10.1098/rstb.2010.0184>.
- Rubia, K., Smith, A.B., Taylor, E., Brammer, M., 2007. Linear age-correlated functional development of right inferior fronto-striato-cerebellar networks during response inhibition and anterior cingulate during error-related processes. *Hum. Brain Mapp.* 28, 1163–1177. <https://doi.org/10.1002/hbm.20347>.
- Rubinov, M., Sporns, O., 2010. Complex network measures of brain connectivity: uses and interpretations. *Neuroimage* 52, 1059–1069. <https://doi.org/10.1016/j.neuroimage.2009.10.003>.
- Satterthwaite, T.D., Wolf, D.H., Loughhead, J., Ruparel, K., Elliott, M.A., Hakonarson, H., Gur, R.E.R.C., Gur, R.E.R.C., 2012. Impact of in-scanner head motion on multiple measures of functional connectivity: relevance for studies of neurodevelopment in youth. *Neuroimage* 60, 623–632. <https://doi.org/10.1016/j.neuroimage.2011.12.063>.
- Scherf, K.S., Behrmann, M., Humphreys, K., Luna, B., 2007. Visual category-selectivity for faces, places and objects emerges along different developmental trajectories. *Dev. Sci.* 10, F15–30. <https://doi.org/10.1111/j.1467-7687.2007.00595.x>.
- Shaw, P., Kabani, N.J., Lerch, J.P., Eckstrand, K., Lenroot, R., Gogtay, N., Greenstein, D., Clasen, L., Evans, A., Rapoport, J.L., Giedd, J.N., Wise, S.P., 2008. Neurodevelopmental trajectories of the human cerebral cortex. *J. Neurosci.* 28, 3586–3594. <https://doi.org/10.1523/JNEUROSCI.5309-07.2008>.
- Shehzad, Z., Kelly, A.M.C., Reiss, P.T., Gee, D.G., Gotimer, K., Uddin, L.Q., Lee, S.H., Margulies, D.S., Roy, A.K., Biswal, B.B., Petkova, E., Castellanos, F.X., Milham, M.P., 2009. The resting brain: unconstrained yet reliable. *Cereb. Cortex* 19, 2209–2229. <https://doi.org/10.1093/cercor/bhn256>.
- Shine, J.M., Poldrack, R.A., 2017. Principles of dynamic network reconfiguration across diverse brain states. *Neuroimage* 1–10. <https://doi.org/10.1016/j.neuroimage.2017.08.010>.
- Shine, J.M., Bissett, P.G., Bell, P.T., Koyejo, O., Balsters, J.H., Gorgolewski, K.J., Moodie, C.A., Poldrack, R.A., 2016. The dynamics of functional brain networks: integrated network states during cognitive task performance. *Neuron* 92, 544–554. <https://doi.org/10.1016/j.neuron.2016.09.018>.
- Shing, Y.L., Lindenberger, U., Diamond, A., Li, S.C., Davidson, M.C., 2010. Memory maintenance and inhibitory control differentiate from early childhood to adolescence. *Dev. Neuropsychol.* 35, 679–697. <https://doi.org/10.1080/87565641.2010.508546>.
- Shirer, W.R., Ryali, S., Rykhlevskaia, E., Menon, V., Greicius, M.D., 2012. Decoding subject-driven cognitive states with whole-brain connectivity patterns. *Cereb. Cortex* 22, 158–165. <https://doi.org/10.1093/cercor/bhr099>.
- Sigala, N., Kusunoki, M., Nimmo-Smith, I., Gaffan, D., Duncan, J., 2008. Hierarchical coding for sequential task events in the monkey prefrontal cortex. *Proc. Natl. Acad. Sci.* 105, 11969–11974. <https://doi.org/10.1073/pnas.0802569105>.
- Simmering, V.R., 2012. The development of visual working memory capacity during early childhood. *J. Exp. Child Psychol.* 111, 695–707. <https://doi.org/10.1016/j.jecp.2011.10.007>.
- Sowell, E.R., Thompson, P.M., Holmes, C.J., Jernigan, T.L., Toga, A.W., 1999. In vivo evidence for post-adolescent brain maturation in frontal and striatal regions. *Nat. Neurosci.* 2, 859–861. <https://doi.org/10.1038/13154>.
- Sowell, E.R., Thompson, P.M., Tessner, K.D., Toga, A.W., 2001. Mapping continued brain growth and gray matter density reduction in dorsal frontal cortex: inverse relationships during postadolescent brain maturation. *J. Neurosci.* 21, 8819–8829. <https://doi.org/10.1523/jneurosci.21-22-08819.2001>.
- Spielberg, J.M., Miller, G.A., Heller, W., Banich, M.T., 2015. Flexible brain network reconfiguration supporting inhibitory control. *Proc. Natl. Acad. Sci.* 112, 10020–10025. <https://doi.org/10.1073/pnas.1500048112>.
- Sporns, O., 2013. Network attributes for segregation and integration in the human brain. *Curr. Opin. Neurobiol.* 23, 162–171. <https://doi.org/10.1016/j.conb.2012.11.015>.
- Sporns, O., Betzel, R.F., 2016. Modular brain networks. *Ssrn* 67, 613–640. <https://doi.org/10.1146/annurev-psych-122414-033634>.
- Steinberg, L., 2005. Cognitive and affective development in adolescence. *Trends Cogn. Sci.* 9, 69–74. <https://doi.org/10.1016/j.tics.2004.12.005>.
- Stevens, M.C., 2016. The contributions of resting state and task-based functional connectivity studies to our understanding of adolescent brain network maturation. *Neurosci. Biobehav. Rev.* 70, 13–32. <https://doi.org/10.1016/j.neubiorev.2016.07.027>.
- Tishby, N., Gat, I., Vaadia, E., Abeles, M., Seidemann, E., Meilijson, I., Bergman, H., 1999. Cortical activity flips among quasi-stationary states. *Proc. Natl. Acad. Sci.* 19, 4595–4608. <https://doi.org/10.1073/pnas.92.19.8616>.
- Vaadia, E., Haalman, I., Abeles, M., Bergman, H., Prut, Y., Slovlin, H., Aertsen, A., 1995. Dynamics of neuronal interactions in monkey cortex in relation to behavioural events. *Nature* 373, 515–518. <https://doi.org/10.1038/373515a0>.
- van den Heuvel, M.P., Sporns, O., 2013. Network hubs in the human brain. *Trends Cogn. Sci.* 17, 683–696. <https://doi.org/10.1016/j.tics.2013.09.012>.
- Váša, F., Romero-García, R., Kitzbichler, M.G., Seidlitz, J., Whitaker, K.J., Vaghi, M.M., Kundu, P., Patel, A.X., Fonagy, P., Dolan, R.J., Jones, P.B., Goodyer, I.M., Vértes, P. E., Bullmore, E.T., 2020. Conservative and disruptive modes of adolescent change in human brain functional connectivity. *Proc. Natl. Acad. Sci.* 117, 3248–3253. <https://doi.org/10.1073/pnas.1906144117>.
- Wang, L., Zhu, C., He, Y., Zang, Y., Cao, Q., Zhang, H., Zhong, Q., Wang, Y., 2009. Altered small-world brain functional networks in children with attention-deficit/hyperactivity disorder. *Hum. Brain Mapp.* 30, 638–649. <https://doi.org/10.1002/hbm.20530>.
- Weil, L.G., Fleming, S.M., Dumontheil, I., Kilford, E.J., Weil, R.S., Rees, G., Dolan, R.J., Blakemore, S.J., 2013. The development of metacognitive ability in adolescence. *Conscious. Cogn.* 22, 264–271. <https://doi.org/10.1016/j.concog.2013.01.004>.
- Xia, M., Wang, J., He, Y., 2013. BrainNet viewer: a network visualization tool for human brain connectomics. *PLoS One* 8. <https://doi.org/10.1371/journal.pone.0068910>.
- Zalecki, C.A., Vaidya, C.J., Gabrieli, J.D.E., Dudukovic, N.M., Bunge, S.A., Elliott, G.R., 2005. Altered neural substrates of cognitive control in childhood ADHD: evidence from functional magnetic resonance imaging. *Am. J. Psychiatry* 162, 1605–1613.
- Zelazo, P.D., Carlson, S.M., 2012. Hot and cool executive function in childhood and adolescence: development and plasticity. *Child Dev. Perspect.* 6, 354–360. <https://doi.org/10.1111/j.1750-8606.2012.00246.x>.
- Zeng, L.L., Shen, H., Liu, L., Wang, L., Li, B., Fang, P., Zhou, Z., Li, Y., Hu, D., 2012. Identifying major depression using whole-brain functional connectivity: a multivariate pattern analysis. *Brain* 135, 1498–1507. <https://doi.org/10.1093/brain/aws059>.